Altered Weddell Sea warm- and dense-water pathways in response to 21st-century climate change

Cara Nissen[1,2], Ralph Timmermann[1], Mathias van Caspel[1], and Claudia Wekerle[1]

[1]Alfred Wegener Institute, Helmholtz-Zentrum für Polar- und Meeresforschung, Bremerhaven, Germany
[2]Department of Atmospheric and Oceanic Sciences and Institute of Arctic and Alpine Research, University of Colorado Boulder, Boulder, CO, USA.

Correspondence: Cara Nissen (cara.nissen@colorado.edu)

Abstract. The transport of water masses with ocean circulation is a key component of the global climate system. In this context, the Filchner Trough in the southern Weddell Sea is critical, as it is a hotspot for the cross-shelf-break exchange of Dense Shelf Water and Warm Deep Water. We present results from Lagrangian particle tracking experiments in a global ocean-sea ice model (FESOM-1.4) which includes ice-shelf cavities and has eddy-permitting resolution on the southern Weddell Sea continental shelf. With backward and forward experiments, we assess changes between a present-day and a future (SSP5-8.5) time slice in the origin of waters reaching the Filchner Ice Shelf front and the fate of waters leaving it. We show that particles reaching the ice-shelf front from the open ocean originate from 173% greater depths by 2100 (median; 776 m as compared to 284 m for the present-day), while waters leaving the cavity towards the open ocean end up at 35% shallower depths (550 m as compared to 850 m for the present-day). Pathways of water leaving the continental shelf increasingly occur in the upper ocean, while the on-shelf flow of waters that might reach the ice shelf cavity, i.e., at deeper layers, becomes more important by 2100. Simultaneously, median transit times between the Filchner Ice Shelf front and the continental shelf break decrease (increase) by 6 (9.5) months in the backward (forward) experiments. In conclusion, our study demonstrates the sensitivity of regional circulation patterns in the southern Weddell Sea to on-going climate change, with direct implications for ice-shelf basal melt rates and local ecosystems.

1 Introduction

The Weddell Sea plays a key role in the global overturning circulation as water masses undergo strong transformations while being transported through this ocean basin (Jacobs, 2004; Marshall and Speer, 2012; Talley, 2013). Its large-scale circulation is dominated by the cyclonic Weddell Gyre, with relatively warm Circumpolar Deep Water (CDW) flowing into the southern Weddell Sea from the east as Warm Deep Water (WDW), gradually upwelling to shallower depths, and ultimately either entering the continental shelf or directly flowing northward along the western flank of the Gyre (Foster and Carmack, 1976; Foldvik et al., 1985; Fahrbach et al., 1994). Part of the WDW mixes with cold Dense Shelf Water (DSW; Jacobs, 2004; Akhoudas et al., 2021), which forms as a result of buoyancy loss on the southern continental shelf (mainly through sea-ice formation; Nicholls et al., 2009; Meredith et al., 2000). The mixing product descends the continental slope into the abyss as

Weddell Sea Deep or Bottom Water (WSDW/WSBW) to form the precursors of Antarctic Bottom Water (AABW; Jacobs, 2004).

The on-shelf transport of WDW in the southern Weddell Sea regulates the access of warm, open-ocean waters to the Filchner Ice Shelf cavity (Darelius et al., 2016) and ultimately controls the ice-shelf basal melt rates and the stability of the Filchner Ice Shelf (Hellmer et al., 2012; Timmermann and Goeller, 2017; Haid et al., 2022; Nissen et al., 2023c). Simultaneously, since WDW is relatively oxygen-poor (Hoppema et al., 1997), the magnitude of its on-shelf transport might directly affect local ecosystems (e.g., Caccavo et al., 2019; Purser et al., 2022). Given that shelf-open ocean exchange is known to be enhanced near troughs and canyons around the Antarctic continent (Morrison et al., 2020), it is unsurprising that observations have confirmed Filchner Trough at ∼30-35°W as a hotspot for the exchange of WDW and DSW across the continental shelf break in the southern Weddell Sea (Fig. 1; Darelius et al., 2016; Ryan et al., 2017; Darelius et al., 2023).

This exchange occurs mostly at the subsurface below 400 m (e.g., Ryan et al., 2020), and we thus largely rely on ship-based or mooring observations for its monitoring. Over recent years, long-term repeat-hydrography expeditions and multi-year mooring deployments have provided great detail about the seasonality and longer-term interannual variability in the on-shelf transport of WDW (Darelius et al., 2016; Ryan et al., 2017, 2020) and the export of Weddell Sea precursors of AABW (Abrahamsen et al., 2019; Darelius et al., 2023; Llanillo et al., 2023), even though for logistical reasons, observation-based assessments are either summer-biased (ship-based observations) or restricted to a small geographical area (mooring-based observations). For example, mooring observations on the eastern side of Filchner Trough have shown that while the on-shelf flow of WDW is generally largest in fall and winter, its magnitude varies substantially from year to year (Ryan et al., 2020). Similarly, the export of AABW precursors from the Weddell Sea undergoes large interannual fluctuations, likely in response to changes upstream on the southern continental shelf (Abrahamsen et al., 2019; Llanillo et al., 2023). Despite the valuable information gained from these observational data sets, exact flow pathways of WDW and DSW in the southern Weddell Sea remain elusive.

Only few modeling studies exist that have assessed circulation or water mass transformations on the high-latitude continental shelves (including those in the Weddell Sea) from a Lagrangian, i.e., flow-following, perspective (Tamsitt et al., 2021; Dawson et al., 2023). Tracking particles that enter the Antarctic continental shelf, Tamsitt et al. (2021) find that WDW in the Weddell Sea spends 1-2 years on average on the continental shelf, after which it is either transformed to a different water mass or leaves the shelf. In a different study using the same model, Dawson et al. (2023) highlight the importance of the Antarctic Slope Current along the continental shelf break for westward transport throughout the Weddell Sea. Yet, as their study focuses exclusively on the connectivity between different Antarctic shelf regions, particle trajectories were excluded from the analysis once the continental shelf break was crossed. Interestingly, for the Weddell Sea, the Filchner Trough region did not stand out in their model as a hotspot of cross-shelf break exchange. This can probably at least partly be attributed to the absence of ice-shelf cavities in their model, which have been suggested to play a key role in controlling Filchner Trough water mass structure and circulation (Darelius and Sallée, 2018; Akhoudas et al., 2020; Janout et al., 2021).

High-resolution models including ice-shelf cavities have shown that processes in the Filchner Trough region will likely become even more important in the future under climate change. In particular, based on Eulerian analysis of model output, existing model projections suggest large changes in DSW properties and shelf-open ocean exchange over the 21st century

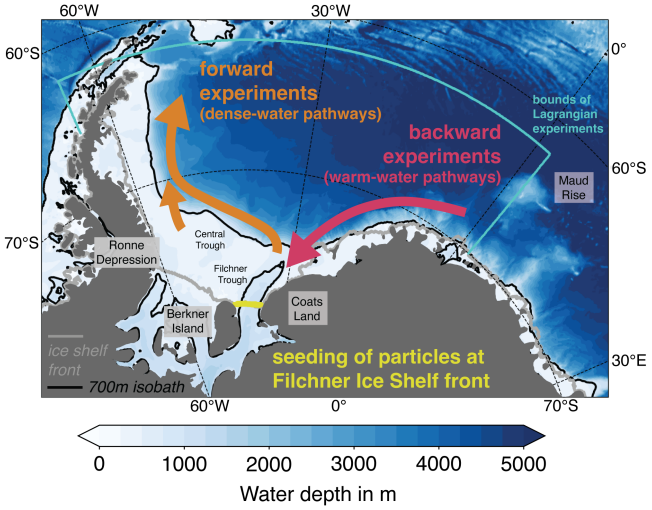

Figure 1. Particles are seeded near the Filchner Ice Shelf front in Filchner Trough (yellow). They are tracked backwards to their origin in the eastern Weddell Sea (red), representing warm-water pathways, and forward to their fate in the western Weddell Sea (orange), representing dense-water pathways. All particles are tracked outside of ice-shelf cavities south of 62°S, east of 65°W, and west of 2°E (cyan bounds). Blue colors display the bottom topography in the area (based on RTopo-2; Schaffer et al., 2016), while the black and grey lines denote the 700 m isobath and the ice-shelf front, respectively.

(Hellmer et al., 2012; Timmermann and Hellmer, 2013; Hellmer et al., 2017; Naughten et al., 2021; Nissen et al., 2022, 2023c). In Hellmer et al. (2012) and Hellmer et al. (2017), a redirected coastal current brings more WDW into the Filchner Ice Shelf cavity, drastically increasing ice-shelf basal melt rates, whereas Timmermann and Hellmer (2013) highlighted the importance of declining sea-ice formation on the continental shelf in triggering this regime shift. Acknowledging that model resolution and the chosen atmospheric forcing scenario impact the susceptibility to change, Nissen et al. (2023c), using newer atmospheric forcing fields, have recently shown a comparable enhancement of the on-shelf transport of WDW at Filchner Trough sill below 400 m for the high-emission scenario SSP5-8.5. In their simulation, the increase is largely driven by an erosion of the cross-shelf break density gradient due to freshening and warming of shelf water masses. In the same model simulation, the export of DSW from the southern Weddell Sea continental shelf becomes less efficient by 2100, which was inferred from the lower density of newly formed DSW, making these waters too light to reach the abyss (Nissen et al., 2022). Overall, while past studies have demonstrated large changes in projected water-mass properties in the Filchner Trough region, which implies changes in circulation, an explicit assessment of the altered pathways of WDW and DSW under 21st-century climate change is still missing.

Here, we perform Lagrangian particle tracking experiments with output from a global ocean-sea ice model with a representation of ice-shelf cavities and eddy-permitting resolution on the Weddell Sea continental shelf (Nissen et al., 2022, 2023c). The aim of our experiments is to compare circulation pathways under present-day conditions and under the high-emission scenario

SSP5-8.5 towards the end of the 21st century. In particular, we assess a) the origin of warm waters reaching the Filchner Ice Shelf front and b) the fate of dense waters leaving the Filchner Ice Shelf cavity (Fig. 1).

2 Methods

2.1 Description of FESOM: model setup and simulations

We use the global ocean–sea ice model FESOM-1.4 (Wang et al., 2014; Danilov et al., 2015) with a representation of ice-shelf cavities (Timmermann et al., 2012) and eddy-permitting resolution on the Weddell Sea continental shelf. The mesh resolution ranges from ∼4 km on the southern Weddell Sea shelf to on average 17 km at the continental shelf break. The mesh has 99 z levels in the vertical. All physical tracers are initialized in 1950 with output from the AWI Climate Model (Semmler et al., 2020), and 3-hourly atmospheric output from the same model is used to force the ocean model at the surface until the year 2100. Semmler et al. (2020) showed that the AWI Climate Model outperforms the CMIP5 multi-model average in representing atmospheric quantities such as winds or temperature for the period 1985-2014 in the Antarctic. Compared to ERA5 reanalysis (Hersbach et al., 2023), simulated near-surface winds in the AWI Climate Model are overall stronger in the Weddell Sea. For this study, we use 20-year daily mean model output from the historical simulation (1990-2009) and the high-emission scenario SSP5-8.5 (2080-2099). The monthly mean output from this model experiment has been evaluated and analyzed in detail in Eulerian space in Nissen et al. (2022, 2023c). Acknowledging that the strength of the Weddell Gyre in the FESOM1.4 simulation is biased low compared to estimates based on Argo floats (Reeve et al., 2019), water-mass distributions and water-mass transformations were shown to overall agree well with observations. In the context of this study, we note the high-density bias of the WDW core in the open ocean, which possibly makes the southern Weddell Sea continental shelf too susceptible for an on-shelf flow of WDW during the 21st century.

2.2 Lagrangian particle tracking

We use the simulated daily mean 3D velocity fields to calculate Lagrangian particle trajectories offline. As all model simulations with FESOM are carried out on an unstructured, triangular mesh (Wang et al., 2014), we use a Langrangian particle tracking algorithm specifically written for this model (Wekerle et al., 2018). The algorithm is based on the following equation:

$$\frac{d\mathbf{x}}{dt} = \mathbf{u}(\mathbf{x}, t) \tag{1}$$

In this equation, **x** is the particle position, and **u** is the velocity field at the same position (both in 3D). Knowing the particle position at time n, its position at time $n + 1$ is

$$\mathbf{x}(t_{n+1}) = \mathbf{x}(t_n) + \int_{t_n}^{t_{n+1}} \mathbf{u}(\mathbf{x}, t)dt. \tag{2}$$

The particle position at time $t_{n+1} = t_n + \delta t$ is computed with the Euler method:

$$\mathbf{x}(t_{n+1}) = \mathbf{x}(t_n) + \mathbf{u}(\mathbf{x}(t_n), t_n)\delta t. \tag{3}$$

The time step is set to one hour for our study. No mixing term is added to the particle motion, i.e., we only analyze the trajectories resulting from the resolved flow field. When a particle reaches the bottom or the continent, it is placed back into the center of the closest ocean grid cell. To increase computational efficiency, we restrict the tracking to our region of interest, i.e., the Weddell Sea between the Filchner Ice Shelf front in the south, 62°S in the north, 65°W in the west, and 2°E in the east.

To assess the origin of waters reaching the Filchner Ice Shelf front and the fate of waters leaving it, we seed particles along a transect at 78°S, i.e., in direct vicinity of the front (Fig. 1). Particles are seeded at 14 locations between Berkner Island in the west and Coats Land in the east and at every 20 m in the vertical, resulting in 596 seeding positions in total. We perform backward experiments to identify the origin of waters in the eastern Weddell Sea and forward experiments to determine the fate of waters in the western Weddell Sea. To that aim, particles are seeded every 10th day in 1990 and 1991 (forward) and 2009 and 2008 (backward) for the historical time period and in 2080 and 2081 (forward) and 2099 and 2098 (backward) for the future time period. We note that we are restricted to these decades due to the availability of daily mean model output and that the two future decades represent a strong climate-change case, with Weddell Sea air temperatures being 5-6°C higher than in the 1990s in our atmospheric forcing fields (Nissen et al., 2023c). In total, 176.416 particles are released. Particle trajectories are computed for the full 20 (19) years or until particles leave the region of interest (see above and Fig. 1), and the position information of the particles is stored twice a day. We note that while the particle tracking code used here does currently not allow for an efficient tracking of particles within ice-shelf cavities, preventing the tracking of any ice-shelf cavity passage in this study, the 3D circulation fields underlying the particle tracking result from the full interaction between the open ocean and the ice-shelf cavity.

In the post-processing, we filter the trajectory data set to focus our analysis on those particles which cross the continental shelf break within their life span. This allows for a more detailed assessment of particles that a) originate from the open ocean and reach the Filchner Ice Shelf front (backward experiments) and b) originate at the Filchner Ice Shelf front and end up in the open ocean (forward experiments). For consistency with Nissen et al. (2023c), the continental shelf break is defined as the 700 m isobath north of 75°S in this study (see black contour in Fig. 1). In total, 8977 (backward, historical), 15166 (backward, future), 5394 (forward, historical), and 5351 (forward, future) trajectories are left for the analysis after the filtering. We note that while these numbers might appear small compared to other published Lagrangian studies (which sometimes use on the order of a million trajectories, see e.g. Tamsitt et al., 2021; Dawson et al., 2023), these earlier studies consider the whole Southern Ocean. In fact, the main finding of our study related to the altered depth distribution of pathways under 21st-century climate change remains qualitatively unchanged when only considering particles seeded in 2009 and 2099 (backward; compare Fig. A1 to Fig. 2) and 1990 and 2080 (forward; compare Fig. A2 to Fig. 6). As a result, we assume the sensitivity of our results is small to adding more particle trajectories to the data set. For a comprehensive assessment of all trajectory positions, we first bin the positions of each trajectory in each of our experiments for a regular 0.5° mesh. Thereafter, we count the particles passing through a given latitude/longitude grid cell at some point (a grid cell can only be counted once for each trajectory), resulting in a visualization of dominant circulation pathways in the Weddell Sea.

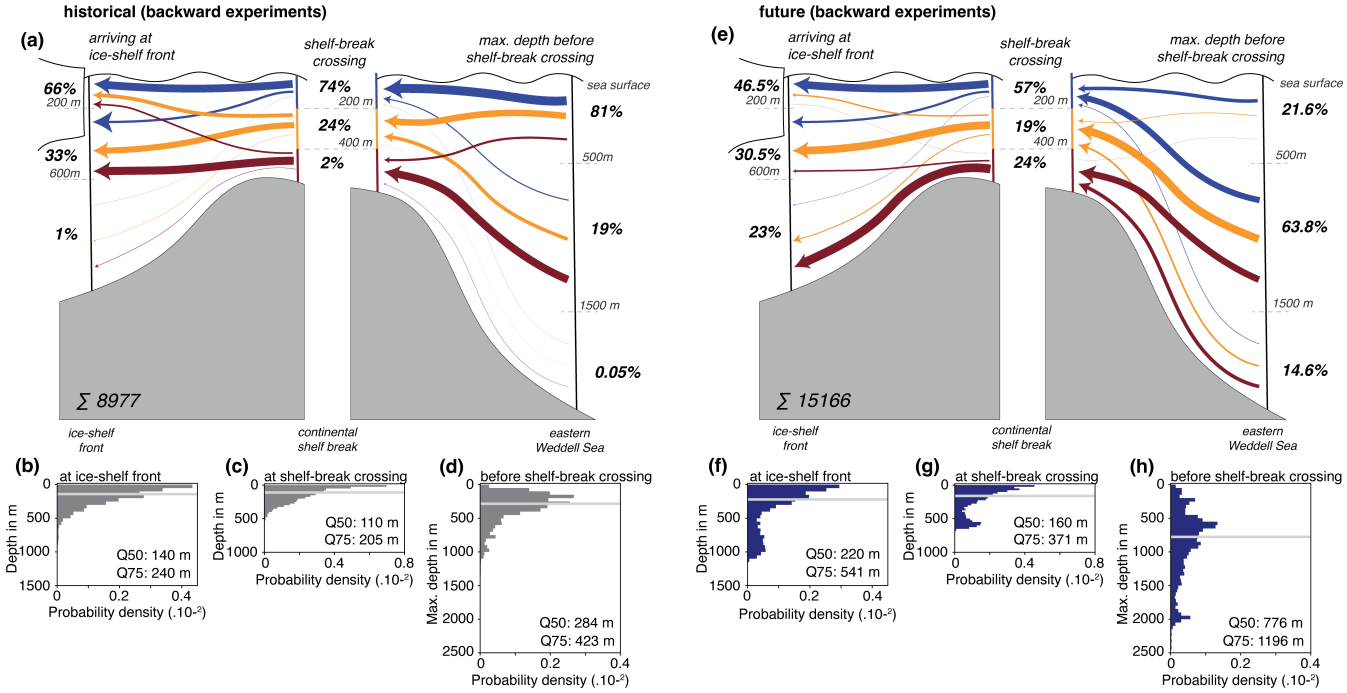

Figure 2. (a) Summary of pathways in the backward tracking experiments for the historical time period of all particles that travel towards the Filchner Ice Shelf front in Filchner Trough from the open ocean. Numbers in percent indicate the distribution of particles over depth at their maximum depth in the eastern Weddell Sea (right; depth intervals separated at 500 m and 1500 m), when entering the continental shelf (middle; separated at 200 m and 400 m), and when reaching the Filchner Ice Shelf front (left; separated at 200 m and 600 m). The arrows are colored depending on the depth level at the shelf-break crossing, and for each color, their line thickness is scaled with the relative importance of different depth intervals for the origin of these waters before the crossing and their fate after the crossing, respectively. The number in the lower left corner denotes the total number of considered particle trajectories. (b)-(d) Probability density distribution for the depth of the particles (b) at seeding at the Filchner Ice Shelf front, (c) at the shelf-break crossing, and (d) at their maximum depth in the eastern Weddell Sea for the backward particle tracking. The symbols Q50 and Q75 refer to the median and the 75th percentile, respectively. (e)-(h) Same as (a)-(d), but for the future time period.

3 Results & Discussion

3.1 Origin of waters reaching the Filchner Ice Shelf front (backward experiments)

For the historical time period, the vast majority of particles reaching the Filchner Ice Shelf front from the open ocean originates from within the uppermost part of the water column. In our backward experiments, 66% of all particles reach the Filchner Ice Shelf front in the top 200 m of the water column, 74% have entered the continental shelf above 200 m, and 81% originate from within the top 500 m offshore (Fig. 2a). Very few particles reaching the Filchner Ice Shelf front originate from below 1500 m in the open ocean (0.05%). Expressed differently, half of the particles reaching the Filchner Ice Shelf front originate

from depths shallower than 284 m in the open ocean, cross the continental shelf break at depths shallower than 110 m, and reach the vicinity of the Filchner Ice Shelf front in the upper 140 m of the water column (Fig. 2b-d). Only 2% of all particles cross the continental shelf break below 400 m, and only 1% reach the Filchner Ice Shelf front below 600 m in the Filchner Trough, implying little inflow of open-ocean waters into the deeper parts of the ice-shelf cavity.

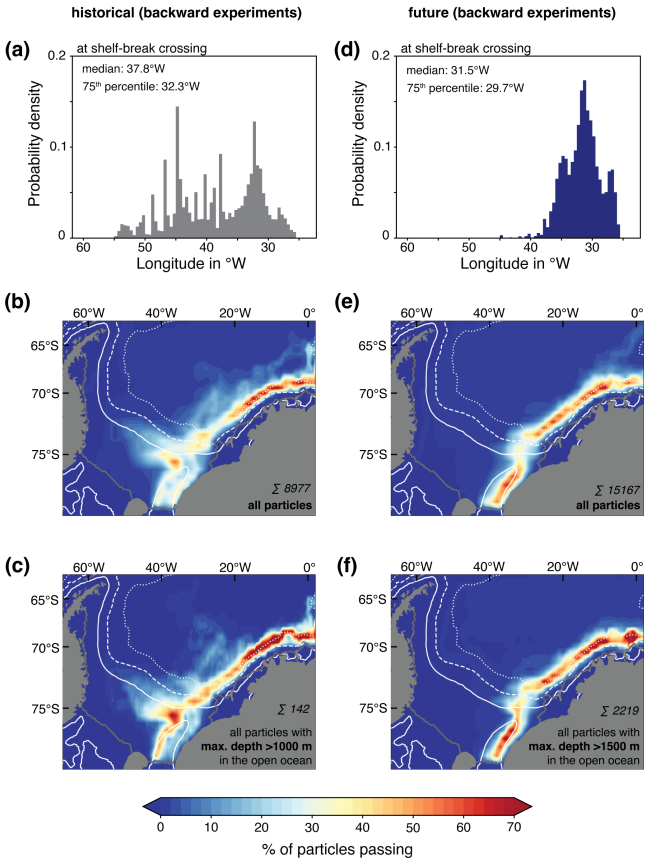

Figure 3. (a) Probability density distribution of the longitude at shelf-break crossing for the backward particle tracking and the historical time period. (b)-(c) Maps denoting how many particles (in %) pass any given location along their backward trajectory for (b) all particles and (c) all particles with a maximum depth of >1000 m in the open ocean. (d)-(f) Same as (a)-(c) but for the future time period and (f) for all particles with a maximum depth of >1500 m in the open ocean. We note that only few particles originate from depths >1500 m in the historical time period (see Fig. 2). The shelf break is here defined as the 700 m isobath north of 75°S (solid white isoline). The other white isolines denote the 2000 m (dashed) and 3500 m (dotted) isobaths, and the dark grey isoline denotes the Filchner Ice Shelf front. In all maps, the total number of assessed trajectories is indicated in the lower right corner.

Particles do not enter the continental shelf at a clearly preferred longitude in the historical time period (left panels in Fig. 3). While half of all particles cross the continental shelf break east and west of 37.8°W, particles enter the shelf as far east as 25°W and as far west as 55°W (Fig. 3a). The spread in longitude is easily visible in the heat maps visualizing the dominant

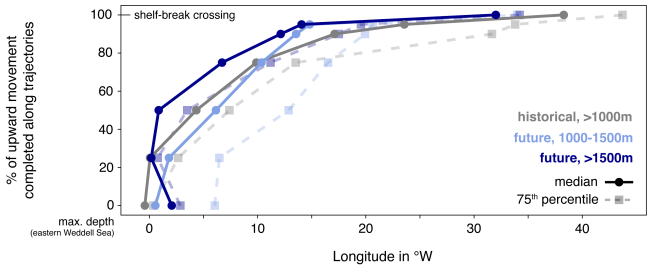

Figure 4. Upward movement of particles in the backward experiments as a function of longitude in % of total upward movement between the location of maximum depth in the eastern Weddell Sea and the depth at the shelf-break crossing (shelf break defined as the 700 m isobath north of 75°S). Solid lines denote the median longitude for a given completed upward movement, and dashed lines the 75th percentile. Grey lines denote all particles for the historical time period originating from >1000 m in the open ocean, and light blue and dark blue lines show all particles for the future time period originating from a depth between 1000-1500 m (light blue) and >1500 m (dark blue).

pathways of all trajectories (Fig. 3b-c). Looking at all particles, our model suggests the general existence of two pathways (Fig. 3b): i) a more direct pathway with particles entering the continental shelf in its easternmost parts and ii) a more indirect route, for which particles enter the shelf further west and are then redirected towards the southeast. While the eastern pathway is frequently confirmed by mooring observations (e.g., Darelius et al., 2016; Ryan et al., 2017, 2020) and a direct pathway from the more western shelf entrances at Central Trough (see Fig. 1) to Ronne Ice Shelf have been inferred from hydrographic observations at the Ronne Ice Shelf front (Nicholls et al., 2003, 2009; Janout et al., 2021; Davis et al., 2022), no observational data set exists to confirm the route from Central Trough to the Filchner Ice Shelf front.

In the open ocean, a pathway along the 3500 m isobath (dotted white isoline in Fig. 3b) is the dominant route towards Filchner Trough, which confirms the key role of the Antarctic Slope Current for westward transport of particles in the area (Thompson et al., 2018; Dawson et al., 2023). Within Filchner Trough, the eastern and western flanks of the trough appear to be equally important pathways towards the Filchner Ice Shelf front in the historical time period. However, for the subset of particles originating from below 1000 m in the open ocean, the path towards the ice-shelf cavity is clearly concentrated along the western flank of Filchner Trough (Fig. 3c), implying a clear east-west distinction in pathways between waters originating from the upper and deep ocean offshore, respectively. In fact, 50% of all particles of deep-ocean origin reach the ice-shelf front below 300 m, whereas this number amounts to only 8% for waters originating from within the top 1000 m in the open ocean, demonstrating that in our model, most particles entering the ice-shelf cavity for the 1990-2009 period flow along the western flank of Filchner Trough and originate from the deep ocean. Acknowledging the small number (142) of the deep-originating particles, half of the particles have completed 50% and 75% of their upward motion between their maximum depth in the eastern Weddell Sea and their depth at shelf-break crossing at 4.3°W and 9.9°W, respectively (grey lines in Fig. 4), implying a key role of upwelling dynamics in the eastern Weddell Sea for the physical-biogeochemical properties of waters reaching the continental shelf and ultimately the Filchner Ice Shelf front (Hoppema et al., 1997).

By the end of the 21st century, more particles reach the Filchner Ice Shelf front at greater depths, while also originating from deeper waters offshore (Fig. 2e). Based on our Lagrangian experiments, 23% of all particles reach the Filchner Ice Shelf front below 600 m under the high-emission scenario SSP5-8.5 (1% for the historical time period), 24% have entered the continental shelf below 400 m (2%), and 15% originate from below 1500 m in the open ocean (0.05%). Overall, almost twice as many particles enter the continental shelf from the open ocean for the future time period (15166) than for the historical time period (8977), reflecting the enhanced on-shelf transport in this area by the end of the 21st century (Nissen et al., 2023c). Under the high-emission scenario, half of the particles reaching the Filchner Ice Shelf front originate from below 776 m in the open ocean, cross the continental shelf break below 160 m, and reach the vicinity of the Filchner Ice Shelf front at depths below 220 m (Fig. 2f-h). Interestingly, a quarter of the particles even originate from below 1196 m (+773 m compared to the historical time period) in the open ocean, cross the continental shelf break below 371 m (+166 m), and reach the vicinity of the Filchner Ice Shelf front at depths below 541 m (+301 m). This illustrates a drastic increase in waters from the deep open ocean reaching the ice-shelf cavity for the future time period, resulting in strong bottom warming and deoxygenation in Filchner Trough and increased ice-shelf basal melt rates (Nissen et al., 2022, 2023c). The overall enhanced future on-shelf transport is facilitated by a reversal of the cross shelf-break density gradient by the end of the 21st century (Nissen et al., 2023c).

Compared to the historical time period, the distribution of longitudes at which particles enter the continental shelf is much more constrained to the southeastern region for the future time period (compare Fig. 3d to panel a). Based on the future backward experiments, particles enter the southern Weddell Sea shelf between 25°W and 40°W (with only few exceptions further west, see Fig. 3d). Half of all particles enter the continental shelf east and west of 31.5°W, respectively. This eastward shift and the overall narrower corridor in which particles enter the continental shelf is reflected by the heat maps (Fig. 3e-f). Looking at all particles, the dominant pathway from the open ocean towards the continental shelf break is more constrained to the continental slope in the future time period, and there are generally fewer trajectories passing through areas north of the 3500 m isobath (Fig. 3e). Yet, albeit not a dominant route, a new source region north of Maud Rise is apparent in the very east of the domain for particles originating from the top 1500 m (see dotted isobath just east of prime meridian; compare Fig. 3e and panel f). While not assessed further in this study, this is likely related to changes in the general circulation in the area, with the Weddell Gyre strengthening overall and shifting southward (Nissen et al., 2022). Within the Filchner Trough, the dominant pathway is now clearly concentrated along its eastern flank for both shallow- and deep-originating particles. With substantially more particles originating from below 1000 m in the future time slice (5069, i.e. 33% of all particles) than in the historical one (142, i.e. 1.5% of all particles), slightly different pathways of upward motion can be identified in our future data set between those particles originating from depths >1500 m and those from between 1000-1500 m (compare light and dark blue lines in Fig. 4). While the trajectory of upward motion for particles originating from between 1000-1500 m largely resembles that of the historical time period (50% and 75% of upward motion completed by 6.1°W and 10.4°W, respectively), the upward motion of the deepest-originating particles occurs further east, with half of the particles having completed 50% and 75% of their upward motion at 0.9°W and 6.7°W, respectively. Altogether, this implies an even larger role for eastern Weddell Sea upwelling dynamics in modulating Filchner Trough water-mass structure and ultimately circulation by the end of the 21st century.

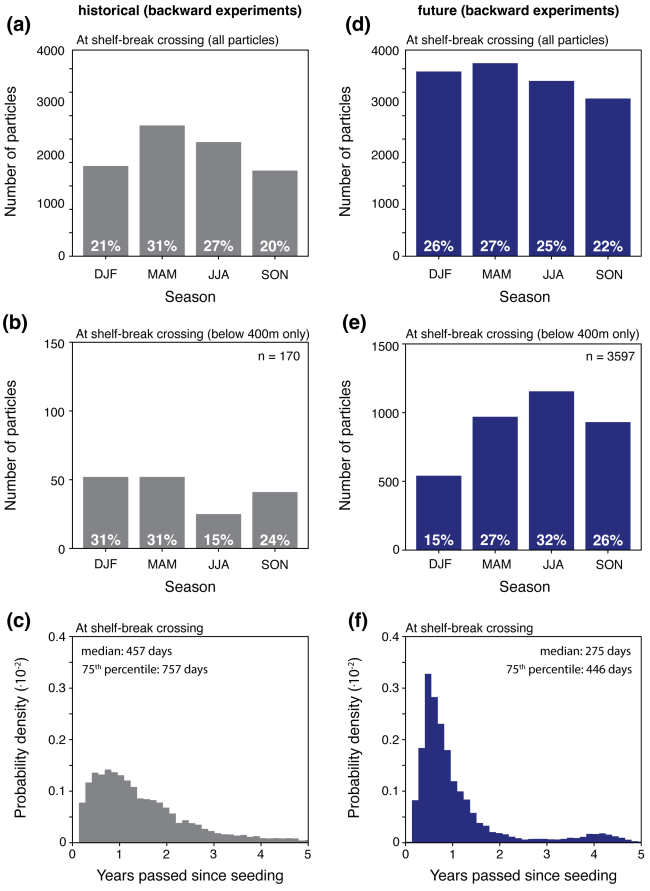

Figure 5. (a) Frequency of the shelf-break crossings for each season for the backward particle tracking for the historical time period. DJF: December-February, MAM: March-May, JJA: June-August, SON: September-November. (b) Same as (a), but for shelf-break crossings below 400 m only. (c) Probability density distribution of time (in years) passed between the seeding of particles at the Filchner Ice Shelf front and the shelf-break crossing for the backward particle tracking and the historical time period. The shelf break is here defined as the 700 m isobath north of 75°S. (d)-(f) Same as (a)-(c), but for the future time period. Note the order-of-magnitude difference between the y-axis limits of panel (b) and (e).

Besides these spatial changes between the historical and the future time period, our Lagrangian experiments also reveal changes in the seasonal timing of shelf-break crossings and the transit time to the Filchner Ice Shelf front. For the historical time period, slightly more of the particles ultimately reaching the Filchner Ice-Shelf front enter the continental shelf in fall and winter (58% for MAM + JJA) than in spring and summer (41% for SON + DJF; Fig. 5a). Interestingly, for those particles entering the shelf below 400 m, i.e., those particles with the highest probability of ultimately entering the Filchner ice-shelf cavity (see red colored arrows in Fig. 1), winter stands out as the season with the least shelf-break crossings (15%; Fig. 5b). Once on the continental shelf, half of the particles take more than 15 months (457 days) until they reach the Filchner Ice Shelf

front (Fig. 5c). Overall, around 39% (73%) of all particles reach the Filchner Ice Shelf front within one year (two years) after crossing the shelf break. This transit time is in broad agreement with findings in Tamsitt et al. (2021, residence time of WDW on the shelf of ∼1-2 years), but substantially longer than the mooring-based estimate by Darelius et al. (2016, ∼two months between 76°S and the ice-shelf front and thus likely less than six months between the continental shelf break and the ice-shelf front). However, when restricting our particle set to the area of mooring deployments in Darelius et al. (2016), i.e., to east of 31°W, thereby excluding the less direct routes towards the ice shelf simulated by our model (see Fig. 3b), a sizeable fraction of Lagrangian particles reaches the Filchner Ice Shelf front within six (26%) and three (9%) months, thus reconciling the two estimates.

For the future time period, the seasonal timing of particles entering the continental shelf is more evenly distributed across seasons (Fig. 5d), implying that the absolute number of shelf-break crossings increases more in spring and summer than in fall and winter relative to the historical period. Yet, for particles entering the shelf below 400 m, there is a disproportionate increase in shelf-break crossings in winter, which represents the season when most particles enter the continental shelf under this high-emission scenario (32%; Fig. 5e). This can likely be attributed to a reduced (or even reversed) density gradient between DSW and WDW in response to enhanced freshwater input and warming, facilitating the on-shelf flow (Ryan et al., 2017; Nissen et al., 2022, 2023c). In addition to these seasonal changes, particles also reach the Filchner Ice Shelf front faster after having entered the continental shelf for the future time period, and half of the particles spend less than 9 months (275 days) on the continental shelf, i.e., 6 months less than for the historical time period (Fig. 5f). This change is even more pronounced for the particles originating from below 1000 m in the open ocean, with a shortening of the median transit time between the shelf-break crossing and the Filchner Ice Shelf front from 26 months (789 days) to a little over 10 months (310 days). As a result, around 66% (88%) of all particles reach the Filchner Ice Shelf front within one year (two years) after crossing the shelf break for the future time period. Of all deep-originating particles (>1000 m), these fractions amount to 62% and 87% (14% and 44% for the historical time period). This reduction in transit time results from a combination of a 34% reduction in the average particle trajectory length and a 7% increase in average current speeds along particle trajectories as compared to the historical time period (not shown).

3.2 Fate of waters leaving the Filchner Ice Shelf front (forward experiments)

For the historical time period, the dominant trajectory pathway between the Filchner Ice Shelf front and the open ocean is in the lower part of the water column, and pathways in the upper ocean are generally of lesser importance. In our forward experiments, almost all particles cross the continental shelf break below 400 m (90%; Fig. 6a), and the majority of the particles along this pathway were seeded below 600 m in the Filchner Trough (red arrows). After leaving the continental shelf, 70% of all particles end up at intermediate depths in the open ocean (500-1500 m) and 13% at depths >1500 m (Fig. 6a). Expressed differently, half of the particles leaving the continental shelf were seeded at the Filchner Ice Shelf front below 660 m, cross the continental shelf break below 600 m, and reach a maximum depth of more than 850 m in the open ocean (Fig. 6b-d). This pathway at depth from the ice-shelf front to the deep open ocean reflects the flow of newly formed dense waters from the continental shelf to the deep ocean abyss.

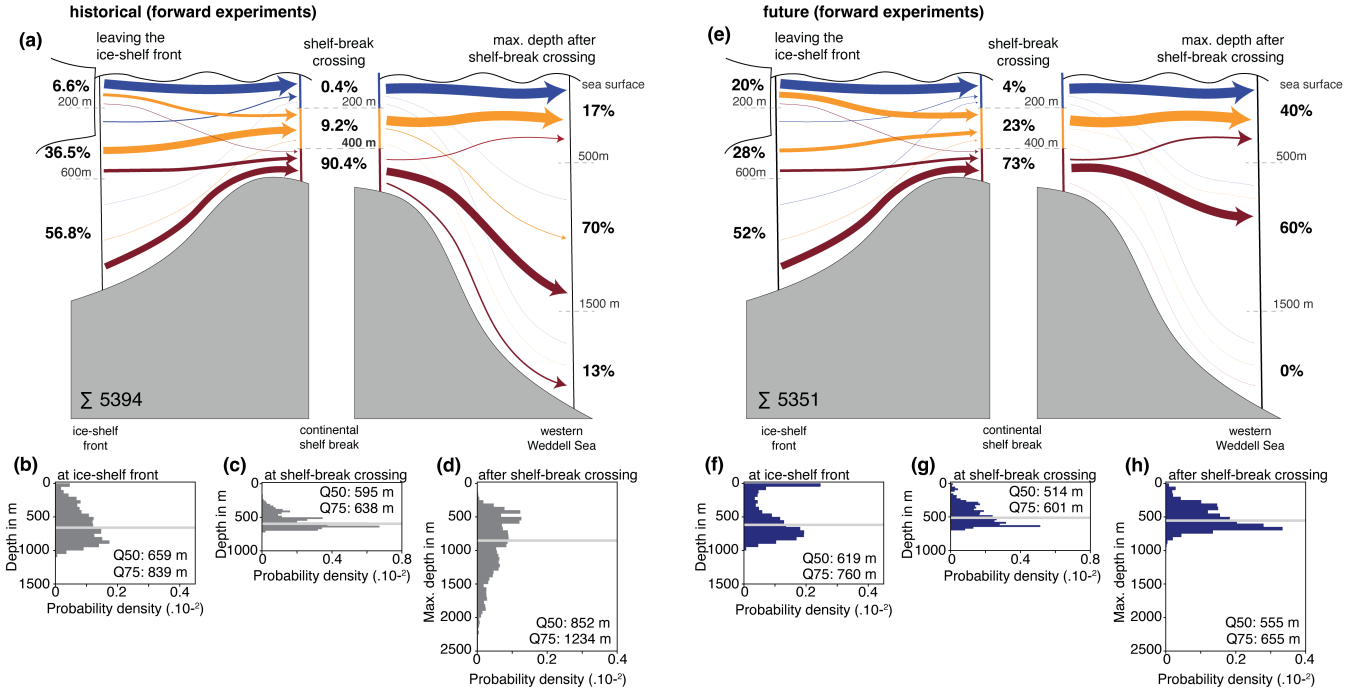

Figure 6. (a) Summary of pathways in the forward tracking experiments for the historical time period of all particles that travel from the Filchner Ice Shelf front in Filchner Trough towards the open ocean. Numbers in percent indicate the distribution of particles over depth when leaving the Filchner Ice Shelf front (left; depth intervals separated at 200 m and 600 m), when leaving the continental shelf (middle; separated at 200 m and 400 m), and at their maximum depth in the western Weddell Sea (right; separated at 500 m and 1500 m). The arrows are colored depending on the depth level at the shelf-break crossing, and for each color, their line thickness is scaled with the relative importance of different depth intervals for the origin of these waters before the crossing and their fate after the crossing, respectively. The number in the lower left corner denotes the total number of considered particle trajectories. (b)-(d) Probability density distribution for the depth of the particles (b) at seeding at the Filchner Ice Shelf front, (c) at the shelf-break crossing, and (d) at their maximum depth in the western Weddell Sea for the forward particle tracking. The symbols Q50 and Q75 refer to the median and the 75th percentile, respectively. (e)-(h) Same as (a)-(d), but for the future time period.

Particles generally leave the continental shelf in one of two sectors for the historical time period. The majority of particles leaves the continental shelf close to Filchner Trough between approximately 33°W and 45°W, while some particles leave the shelf in more western parts (west of 55°W; left window in Fig. 7a). The particle trajectory on the continental shelf and the fate of particles in the open ocean differ depending on the exit route. Looking at all particles, the dominance of the Filchner Trough pathway is obvious (Fig. 7b), and particles are predominantly transported towards the continental shelf break along the eastern flank of the trough, in agreement with the observational data presented in Darelius et al. (2014) and Ryan et al. (2017). The less important western exit route first transports particles towards Ronne Depression (see Fig. 1) and then northwards off the continental shelf. Separately assessing particles which end up at depths >1500 m in the open ocean, the absence of the western

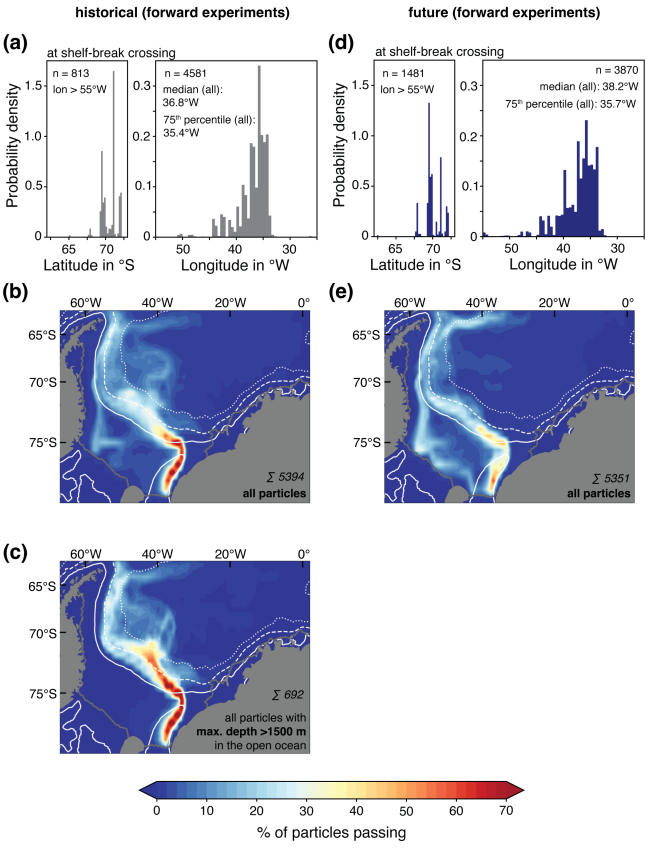

Figure 7. (a) Probability density distribution of the latitude and longitude at shelf-break crossing for particles crossing west and east of 55°W, respectively, for the forward particle tracking and the historical time period. (b)-(c) Maps denoting how many particles (in %) pass any given location along their forward trajectory for (b) all particles and (c) all particles ending up at a depth of >1500 m in the open ocean. (d)-(e) Same as (a)-(b) but for the future time period. The shelf break is here defined as the 700 m isobath north of 75°S (solid white isoline). The other white isolines denote the 2000 m (dashed) and 3500 m (dotted) isobaths, and the dark grey isoline denotes the Filchner Ice Shelf front. In all maps, the total number of assessed trajectories is indicated in the lower right corner. A panel (f) does not exist because no particles originating from Filcher Ice Shelf end up in a depth >1500 m.

route in Fig. 7c demonstrates that this pathway is restricted to particles remaining in the upper ocean and does therefore not display a second exit route for newly formed dense waters. Instead, it indicates that some of the water leaving Filchner Ice Shelf cavity may recirculate on the continental shelf and re-enter the cavity through Ronne Trough (such trajectories were not tracked with our experimental setup, see Methods, but it is seems probable that they exist).

In the open ocean, some particles split off close to 40°W to flow towards the deep central Weddell Sea basin (especially true for particles reaching a maximum depth of >1500 m in the open ocean; Fig. 7c), while most particles continue to flow towards the northwest along the continental slope and enter the deep ocean near the transition to Scotia Sea, a known exit route for newly formed dense waters from the Weddell Sea (Abrahamsen et al., 2019; Llanillo et al., 2023). It seems plausible that

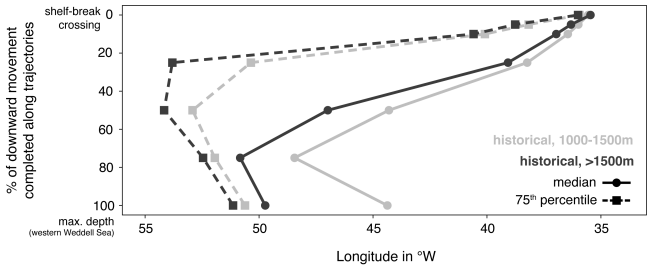

Figure 8. Downward movement of particles in the forward experiments as a function of longitude between the depth at the shelf-break crossing and location of maximum depth in the western Weddell Sea (in % of total downward movement; shelf break defined as the 700 m isobath north of 75°S). Solid lines denote the median longitude for a given completed downward movement, and dashed lines the 75th percentile. Light grey lines denote all particles for the historical time period with a maximum depth in the open ocean between 1000-1500 m, and dark grey lines show all particles for the historical time period with a maximum depth of >1500 m. Note that the future time period is not shown here as very few particles descend to below 1000 m (see also Figs. 6 and 7).

the split at 40°W represents two variants of WSBW originating from the southeastern shelf, with the northwestward-flowing variant interacting with WSBW originating from the continental shelf in front of Larsen Ice Shelf on its way north (Absy et al., 2008). During their transport along the western flank of the Weddell Gyre, the particles gradually descend into the deeper ocean (Fig. 8). Half (three quarters) of the particles have completed 50% (25%) of the total downward movement between their depth at the shelf-break crossing and their maximum depth in the open ocean within ∼10 (15) degrees in longitude after leaving the continental shelf close to 36°W. As a result of the north-south orientation of the continental slope in the western Weddell Sea (see e.g., Fig. 7), the remaining 50% (75%) are associated with less longitudinal displacement. Altogether, this illustrates the importance of the entire southern and southwestern continental slope for the downward transport of waters originating in the Filchner Trough.

By the end of the 21st century, the dominant trajectory pathways shift to shallower depths in our forward experiments. In particular, a larger fraction of particles leaves the continental shelf above 400 m (27% as compared to <10% for the historical time period; Fig. 6). Most importantly, only 60% of all particles reach a depth of more than 500 m in the open ocean (83% for the historical time period), and not a single particle ends up below 1500 m. For this scenario, half of the particles leaving the continental shelf were seeded below 620 m (40 m shallower than for to the historical time period), leave the continental shelf below 510 m (∼80 m shallower), and end up below 550 m (∼300 m shallower) in the open ocean. The change is even more pronounced for the 75th percentile, with the maximum depth being 579 m shallower than for the historical time period (655 m vs. 1234 m; Fig. 6d and h). Overall, this reflects the reduced ability of newly formed dense waters to reach the deep ocean in the future time slice under this high-emission scenario, which was also inferred from changes in the Eulerian density fields in Nissen et al. (2022). The reduced density of newly formed dense waters is mainly caused by the freshening of waters on the continental shelf as a result of reduced sea-ice formation and enhanced ice-shelf basal melt and results in reduced ventilation of bottom waters along the Weddell Sea continental slope (Nissen et al., 2022).

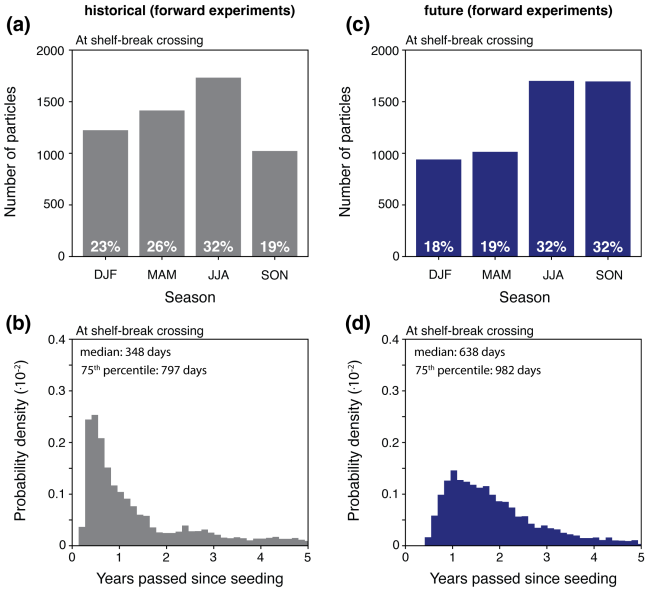

Figure 9. (a) Frequency of the shelf-break crossings for each season for the forward particle tracking for the historical time period. DJF: December-February, MAM: March-May, JJA: June-August, SON: September-November. (b) Probability density distribution of time (in years) passed between the seeding of particles at the Filchner Ice Shelf front and the shelf-break crossing for the forward particle tracking and the historical time period. The shelf break is here defined as the 700 m isobath north of 75°S. (c)-(d) Same as (a)-(b), but for the future time period.

To a first degree, there is rather little change in the longitude corridors in which particles leave the continental shelf between the historical and the future time period. The longitude at which half of the particles cross the continental shelf break shifts westward by 1.4° (from 36.8°W to 38.2°W; compare Fig. 7a and d), illustrating a slightly increased importance of the western exit route under the high-emission scenario (see left windows in Fig. 7a and d). Given that the western corridor is generally associated with particles leaving at shallower depths than for the exit route at Filchner Trough (see Fig. 7b and c), the westward shift is consistent with the overall shift towards particles crossing the shelf break at shallower depths in the future time slice (Fig. 6). The heat map further illustrates this point, as it shows a higher percentage of particles passing the Ronne Depression area before leaving the continental shelf (Fig. 7e). As mentioned already, no particles originating from Filchner Ice Shelf end up at a depth greater than 1500 m in this simulation.

Like for the backward experiments, the forward experiments also reveal changes in the transit times to the continental shelf break and the seasonal timing of its crossing. In the historical time, fall and winter are the seasons with the most frequent offshore transport of particles (58% for MAM + JJA), while the other seasons contribute less (42% for SON + DJF; Fig. 9a). Until leaving the continental shelf, half of the particles spend less than 12 months (348 days) on the continental shelf (Fig. 9b). Overall, around 52% (73%) of all particles leave the continental shelf within one year (two years) after seeding at the Filchner

Ice Shelf front. This is in agreement with observation-based estimates of a residence time of waters within Filchner Trough of less than two years (Nøst and Østerhus, 1985) and 2-7 months (Darelius et al., 2014), respectively.

In the future simulation, there is a clear change in the seasonality of offshore particle transport. With the total number of particles remaining virtually unchanged, spring (SON) contributes as much as winter (JJA) to the offshore transport of particles under the high-emission scenario (32%; Fig. 9c). Acknowledging that, similar to the backward experiments, local changes in the density structure also play a role, we here assume that this change in seasonality is largely the result of the changing pathways from the Filchner Ice Shelf front to the continental shelf break (compare Figs. 7b and e). In contrast to the backward experiments, there is an increase for the future time slice in the transit times of particles between the Filchner Ice Shelf front and the crossing of the continental shelf break. Considering all particles, half of them spend up to 21 months (638 days) on the continental shelf, i.e., around 10 months longer than for the historical time period (Fig. 9d). Overall, only around 17% (59%) of all particles leave the continental shelf within one year (two years) after seeding at the Filchner Ice Shelf front. The increase in the transit time results from a combination of a 9% increase in the average particle trajectory length and a 12% reduction in average current speeds along particle trajectories as compared to the historical time period (not shown).

4 Limitations and caveats

The main limitation surrounding our findings concerns choices in the model setup and approximations in the model equations. In particular, the use of the hydrostatic approximation in FESOM1.4 means that convective processes, such as those involved in dense-water formation, are not explicitly resolved (Marshall et al., 1997; Wang et al., 2014). While the impact of convection is parameterized for tracer fields (Wang et al., 2014), its effect is not included in the velocity fields underlying our Lagrangian particle tracking experiments. While some authors have included random mixing terms in their Langrangian studies to at least partially account for parameterized vertical mixing processes (e.g., Dawson et al., 2023), we note that our model is able to render plausible, realistic dense-water pathways from the current field alone. Specifically, the maximum depth that particles reach after leaving the continental shelf in our forward experiment exceeds 3000 m, and $\sim$13% of particles reach a depth $>$1500 m for the historical period. This suggests that even with the hydrostatic approximation in FESOM1.4, processes representation is likely sufficient for our application, even though the maximum depth of simulated particles offshore is likely under- rather than overestimated. Further, we note that despite using a z-coordinate in the vertical, our particle trajectories do not display stair-case behavior, suggesting a realistic representation of vertical movement. Lastly, by using daily-averaged velocity fields to advect Lagrangian particles, we acknowledge that the mesoscale is not fully resolved. Yet, as all of these points can be expected to impact both time slices in a similar manner, we assume the qualitative results of our study to only be marginally affected by these limitations.

5 Conclusions

Using backward and forward Lagrangian particle tracking experiments for a historical and a future time slice focusing on the origin and fate of waters at the Filchner Ice Shelf front in the southern Weddell Sea, we demonstrate that for the high-emission scenario SSP5-8.5, pathways of both Warm Deep Water and Dense Shelf Water are altered by the end of the 21st century. While the less efficient export of newly formed Dense Shelf Water to the abyss reflects the substantial projected freshening and warming of this water mass by 2100 (Nissen et al., 2022), this change also results in upper ocean circulation pathways becoming more important for the transit from the Filchner Ice Shelf front to the open ocean. Simultaneously, waters reaching the Filchner Ice Shelf front increasingly originate from new, deeper source regions in the eastern Weddell Sea, possibly changing water-mass properties and thereby further modifying local shelf circulation and the transit time to the Filchner Ice Shelf front.

Future work should investigate in more detail how upwelling dynamics in the eastern Weddell Sea relate to cross-shelf-break exchange near Filchner Trough, as our results imply that processes upstream directly impact water-mass properties in the Filchner Trough. Even though the forward and backward trajectories are not computed for the exact same years in our study, mirrored future change in the two experiments, e.g. regarding transit times between the ice-shelf front and the continental shelf break, indicate systematic circulation changes in Filchner Trough. As such changes have direct implications for the export of newly formed Dense Shelf Water (Nissen et al., 2022), the access of Warm Deep Water to the ice-shelf cavity (Hellmer et al., 2012; Nissen et al., 2023c), and the life cycle of some key local species relying on Filchner Trough circulation (e.g., the Antarctic silverfish, see Caccavo et al., 2019), sustained monitoring of ocean circulation in this area is necessary.

Code and data availability. The Lagrangian particle trajectories are deposited at doi: 10.5281/zenodo.8051366 (Nissen, 2023). Full model fields underlying the analysis are deposited at the World Data Center for Climate (WDCC) at DKRZ under doi 10.26050/WDCC/FESOM14-REcoM2_A_hist_vA_vC (1990-2009; Nissen et al., 2023a) and doi 10.26050/WDCC/FESOM14-REcoM2_A_s585_vA_vC (2080-2099; Nissen et al., 2023b). The particle tracking code and python analysis scripts can be made available upon request to the corresponding author.

Appendix A: Sensitivity of results to the number of particles

To investigate the sensitivity of our results to the number of particles, we repeated the core diagnostics with a reduced-number subset of our float data set. Specifically, we ran the present-day experiments with only particles in 1990 for the forward and in 2008 for the backward run. Similarly, for the future projections, we only include particles seeded in 2080 (forward) and 2099 (backward). We find that the results remain qualitatively unchanged compared to the full-dataset analysis (compare Figs. A1 and A2 below to Figs. 2 and 6 in the main text).

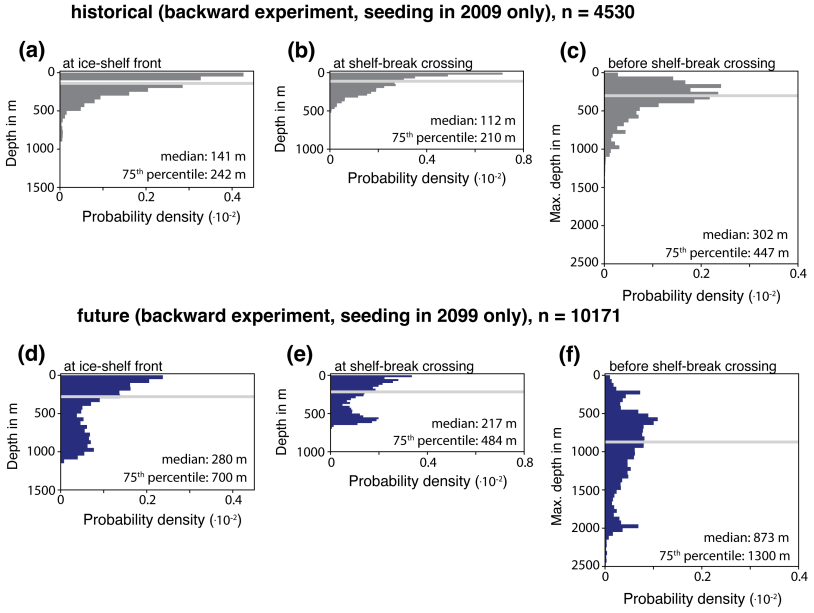

Figure A1. Sensitivity of results in backward tracking experiments to particle number: (a)-(c) Probability density distribution for the depth of the particles (a) at seeding at the Filchner Ice Shelf front, (b) at the shelf-break crossing, and (c) at their maximum depth in the eastern Weddell Sea. Panels (a)-(c) show the same quantities as in Fig. 2 (b)-(d), but for seeding in 2009 only. (d)-(f) Same as (a)-(c), but for the future time period. Panels (d)-(f) show the same quantities as in Fig. 2 (f)-(h), but for seeding in 2099 only.

Author contributions. CN conceived the study, ran the Eulerian and Lagrangian model experiments, performed the analysis, and wrote the first version of the manuscript. RT and CW developed the particle tracking code. All authors contributed to the interpretation of the findings and to the writing of the manuscript.

Competing interests. The authors declare that they have no conflict of interest.

Acknowledgements. We are grateful to Judith Hauck and Özgür Gürses for their help in setting up the Eulerian model experiments and to Uta Menzel for programming the original version of our Lagrangian particle tracking toolbox. This project has received funding from the European Union's Horizon 2020 research and innovation programme under grant agreement No 820989 (project COMFORT) and support from the Helmholtz Climate Initiative REKLIM (Regional Climate Change), a joint research project of the Helmholtz Association of German research centres (HGF). CW received funding from the Federal Ministry of Education and Research in Germany (BMBF) through the research program "GROCE2" (FKZ 03F0855A). MvC acknowledges funding from the Horizon Europe Funding Programme for research and innovation under grant agreement No 101060452 (project OCEAN:ICE). The work reflects only the authors' view; the European Commission and their executive agency are not responsible for any use that may be made of the information the work contains. Computing resources were provided by the North-German Supercomputing Alliance (HLRN) project hbk00079.

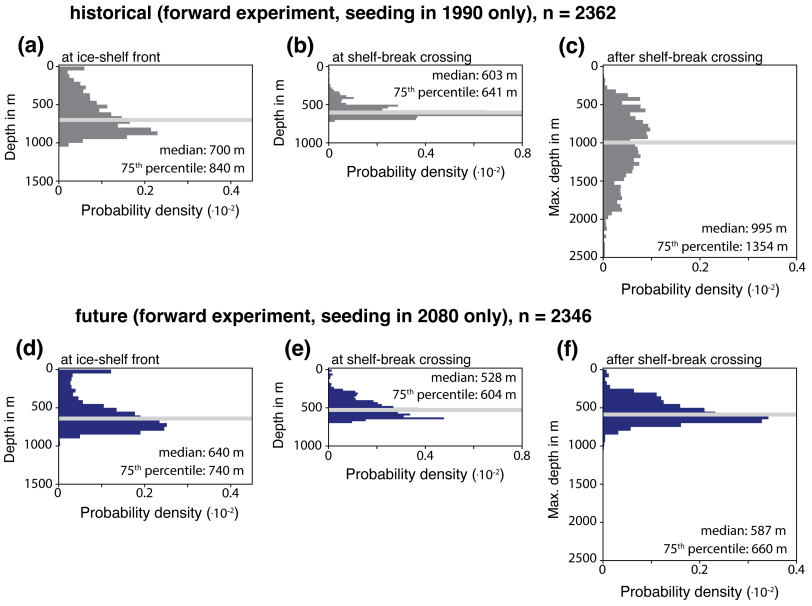

Figure A2. Sensitivity of results in forward tracking experiments to particle number: (a)-(c) Probability density distribution for the depth of the particles (a) at seeding at the Filchner Ice Shelf front, (b) at the shelf-break crossing, and (c) at their maximum depth in the western Weddell Sea. Panels (a)-(c) show the same quantities as in Fig. 6 (b)-(d), but for seeding in 1990 only. (d)-(f) Same as (a)-(c), but for the future time period. Panels (d)-(f) show the same quantities as in Fig. 6 (f)-(h), but for seeding in 2080 only.

References

Abrahamsen, E. P., Meijers, A. J. S., Polzin, K. L., Garabato, A. C. N., King, B. A., Firing, Y. L., Sallée, J.-b., Sheen, K. L., Gordon, A. L., Huber, B. A., and Meredith, M. P.: Stabilization of dense Antarctic water supply to the Atlantic Ocean overturning circulation, Nature Climate Change, 9, https://doi.org/10.1038/s41558-019-0561-2, 2019.

Absy, J., Schröder, M., Muench, R., and Hellmer, H.: Early summer thermohaline characteristics and mixing in the western Weddell Sea, Deep Sea Research Part II: Topical Studies in Oceanography, 55, 1117–1131, https://doi.org/10.1016/j.dsr2.2007.12.023, 2008.

Akhoudas, C., Sallée, J.-B., Reverdin, G., Aloisi, G., Benetti, M., Vignes, L., and Gelado, M.: Ice Shelf Basal Melt and Influence on Dense Water Outflow in the Southern Weddell Sea, Journal of Geophysical Research: Oceans, 125, 1–19, https://doi.org/10.1029/2019JC015710, 2020.

Akhoudas, C., Sallée, J.-B., Haumann, F. A., Meredith, M. P., Garabato, A. N., Reverdin, G., Jullion, L., Aloisi, G., Benetti, M., Leng, M. J., and Arrowsmith, C.: Ventilation of the abyss in the Atlantic sector of the Southern Ocean, Scientific Reports, 11, 6760, https://doi.org/10.1038/s41598-021-86043-2, 2021.

Caccavo, J., Ashford, J., Ryan, S., Papetti, C., Schröder, M., and Zane, L.: Spatial structuring and life history connectivity of Antarctic silverfish along the southern continental shelf of the Weddell Sea, Marine Ecology Progress Series, 624, 195–212, https://doi.org/10.3354/meps13017, 2019.

Danilov, S., Wang, Q., Timmermann, R., Iakovlev, N., Sidorenko, D., Kimmritz, M., Jung, T., and Schröter, J.: Finite-Element Sea Ice Model (FESIM), version 2, Geoscientific Model Development, 8, 1747–1761, https://doi.org/10.5194/gmd-8-1747-2015, 2015.

Darelius, E. and Sallée, J. B.: Seasonal Outflow of Ice Shelf Water Across the Front of the Filchner Ice Shelf, Weddell Sea, Antarctica, Geophysical Research Letters, 45, 3577–3585, https://doi.org/10.1002/2017GL076320, 2018.

Darelius, E., Makinson, K., Daae, K., Fer, I., Holland, P. R., and Nicholls, K. W.: Hydrography and circulation in the Filchner Depression, Weddell Sea, Antarctica, Journal of Geophysical Research: Oceans, 119, 5797–5814, https://doi.org/10.1002/2014JC010225, 2014.

Darelius, E., Fer, I., and Nicholls, K. W.: Observed vulnerability of Filchner-Ronne Ice Shelf to wind-driven inflow of warm deep water, Nature Communications, 7, 12 300, https://doi.org/10.1038/ncomms12300, 2016.

Darelius, E., Daae, K., Dundas, V., Fer, I., Hellmer, H. H., Janout, M., Nicholls, K. W., Sallée, J.-b., and Østerhus, S.: Observational evidence for on-shelf heat transport driven by dense water export in the Weddell Sea, Nature Communications, 14, 1022, https://doi.org/10.1038/s41467-023-36580-3, 2023.

Davis, P. E. D., Jenkins, A., Nicholls, K. W., Dutrieux, P., Schröder, M., Janout, M. A., Hellmer, H. H., Templeton, R., and McPhail, S.: Observations of Modified Warm Deep Water Beneath Ronne Ice Shelf, Antarctica, From an Autonomous Underwater Vehicle, Journal of Geophysical Research: Oceans, 127, https://doi.org/10.1029/2022JC019103, 2022.

Dawson, H. R. S., Morrison, A. K., England, M. H., and Tamsitt, V.: Pathways and timescales of connectivity around the Antarctic continental shelf, Journal of Geophysical Research: Oceans, p. 14011, https://doi.org/10.1029/2022JC018962, 2023.

Fahrbach, E., Rohardt, G., Schröder, M., and Strass, V.: Transport and structure of the Weddell Gyre, Annales Geophysicae, 12, 840–855, https://doi.org/10.1007/s00585-994-0840-7, 1994.

Foldvik, A., Gammelsrød, T., and Tørresen, T.: Circulation and water masses on the southern Weddell Sea shelf, Oceanology of the Antarctic Continental Shelf, Vol. 43, 5-20, American Geophysical Union, 1985.

Foster, T. D. and Carmack, E. C.: Frontal zone mixing and Antarctic Bottom water formation in the southern Weddell Sea, Deep Sea Research and Oceanographic Abstracts, 23, 301–317, https://doi.org/10.1016/0011-7471(76)90872-X, 1976.

Haid, V., Timmermann, R., Gürses, Ö., and Hellmer, H. H.: On the drivers of regime shifts in the Antarctic marginal seas, EGUsphere, 2022, 1–18, https://doi.org/10.5194/egusphere-2022-1044, 2022.

Hellmer, H. H., Kauker, F., Timmermann, R., Determann, J., and Rae, J.: Twenty-first-century warming of a large Antarctic ice-shelf cavity by a redirected coastal current, Nature, 485, 225–228, https://doi.org/10.1038/nature11064, 2012.

Hellmer, H. H., Kauker, F., Timmermann, R., and Hattermann, T.: The Fate of the Southern Weddell Sea Continental Shelf in a Warming Climate, Journal of Climate, 30, 4337–4350, https://doi.org/10.1175/JCLI-D-16-0420.1, 2017.

Hersbach, H., Bell, B., Berrisford, P., Biavati, G., Horányi, A., Muñoz Sabater, J., Nicolas, J., Peubey, C., Radu, R., Rozum, I., Schepers, D., Simmons, A., Soci, C., Dee, D., and Thépaut, J.-N.: ERA5 hourly data on single levels from 1940 to present. Copernicus Climate Change Service (C3S) Climate Data Store (CDS), https://doi.org/10.24381/cds.adbb2d47; accessed on 06-Nov-2023, 2023.

Hoppema, M., Fahrbach, E., and Schröder, M.: On the total carbon dioxide and oxygen signature of the Circumpolar Deep Water in the Weddell Gyre, Oceanologica Acta, 20, 783–798, 1997.

Jacobs, S. S.: Bottom water production and its links with the thermohaline circulation, Antarctic Science, 16, 427–437, https://doi.org/10.1017/S095410200400224X, 2004.

Janout, M. A., Hellmer, H. H., Hattermann, T., Huhn, O., Sültenfuss, J., Østerhus, S., Stulic, L., Ryan, S., Schröder, M., and Kanzow, T.: FRIS Revisited in 2018: On the Circulation and Water Masses at the Filchner and Ronne Ice Shelves in the Southern Weddell Sea, Journal of Geophysical Research: Oceans, 126, 1–19, https://doi.org/10.1029/2021JC017269, 2021.

Llanillo, P. J., Kanzow, T., Janout, M. A., and Rohardt, G.: The Deep-Water Plume in the Northwestern Weddell Sea, Antarctica: Mean State, Seasonal Cycle and Interannual Variability Influenced by Climate Modes, Journal of Geophysical Research: Oceans, 128, 1–22, https://doi.org/10.1029/2022JC019375, 2023.

Marshall, J. and Speer, K.: Closure of the meridional overturning circulation through Southern Ocean upwelling, Nature Geoscience, 5, 171–180, https://doi.org/10.1038/ngeo1391, 2012.

Marshall, J., Hill, C., Perelman, L., and Adcroft, A.: Hydrostatic, quasi-hydrostatic, and nonhydrostatic ocean modeling, Journal of Geophysical Research: Oceans, 102, 5733–5752, https://doi.org/10.1029/96JC02776, 1997.

Meredith, M. P., Locarnini, R. A., Van Scoy, K. A., Watson, A. J., Heywood, K. J., and King, B. A.: On the sources of Weddell Gyre Antarctic Bottom Water, Journal of Geophysical Research: Oceans, 105, 1093–1104, https://doi.org/10.1029/1999JC900263, 2000.

Morrison, A. K., Hogg, A. M., England, M. H., and Spence, P.: Warm Circumpolar Deep Water transport toward Antarctica driven by local dense water export in canyons, Science Advances, 6, eaav2516, https://doi.org/10.1126/sciadv.aav2516, 2020.

Naughten, K. A., De Rydt, J., Rosier, S. H. R., Jenkins, A., Holland, P. R., and Ridley, J. K.: Two-timescale response of a large Antarctic ice shelf to climate change, Nature Communications, 12, 1991, https://doi.org/10.1038/s41467-021-22259-0, 2021.

Nicholls, K. W., Padman, L., Schröder, M., Woodgate, R., Jenkins, A., and Østerhus, S.: Water mass modification over the continental shelf north of Ronne Ice Shelf, Antarctica, Journal of Geophysical Research, 108, 3260, https://doi.org/10.1029/2002JC001713, 2003.

Nicholls, K. W., Østerhus, S., Makinson, K., Gammelsrød, T., and Fahrbach, E.: Ice-ocean processes over the continental shelf of the southern Weddell Sea, Antarctica: A review, Reviews of Geophysics, 47, RG3003, https://doi.org/10.1029/2007RG000250, 2009.

Nissen, C.: FESOM-REcoM model data: Lagrangian particle trajectories, Zenodo, https://doi.org/10.5281/zenodo.8051366, 2023.

Nissen, C., Timmermann, R., Hoppema, M., Gürses, Ö., and Hauck, J.: Abruptly attenuated carbon sequestration with Weddell Sea dense waters by 2100, Nature Communications, 13, 3402, https://doi.org/10.1038/s41467-022-30671-3, 2022.

Nissen, C., Hauck, J., Hoppema, M., Timmermann, R., and Gürses, O.: HighRes_highLat_SO FESOM1.4-REcoM2 model simulations to project future change in the coupled physical-biogeochemical system simA historical variableAtmCO2 variableClimate. World Data Center for Climate (WDCC) at DKRZ, https://doi.org/10.26050/WDCC/FESOM14-REcoM2_A_hist_vA_vC, 2023a.

Nissen, C., Hauck, J., Hoppema, M., Timmermann, R., and Gürses, O.: HighRes_highLat_SO FESOM1.4-REcoM2 model simulations to project future change in the coupled physical-biogeochemical system simA SSP585 variableAtmCO2 variableClimate. World Data Center for Climate (WDCC) at DKRZ, https://doi.org/10.26050/WDCC/FESOM14-REcoM2_A_s585_vA_vC, 2023b.

Nissen, C., Timmermann, R., Hoppema, M., and Hauck, J.: A Regime Shift on Weddell Sea Continental Shelves with Local and Remote Physical and Biogeochemical Implications is Avoidable in a 2°C Scenario, Journal of Climate, 36, 6613–6630, https://doi.org/10.1175/JCLI-D-22-0926.1, 2023c.

Nøst, O. A. and Østerhus, S.: Impact of Grounded Icebergs on the Hydrographic Conditions Near the Filchner Ice Shelf, in: Ocean, Ice, and Atmosphere: Interactions at the Antarctic Continental Margin, pp. 267–284, American Geophysical Union (AGU), https://doi.org/https://doi.org/10.1029/AR075p0267, 1985.

Purser, A., Hehemann, L., Boehringer, L., Tippenhauer, S., Wege, M., Bornemann, H., Pineda-Metz, S. E., Flintrop, C. M., Koch, F., Hellmer, H. H., Burkhardt-Holm, P., Janout, M., Werner, E., Glemser, B., Balaguer, J., Rogge, A., Holtappels, M., and Wenzhoefer, F.: A vast icefish breeding colony discovered in the Antarctic, Current Biology, 32, 842–850.e4, https://doi.org/10.1016/j.cub.2021.12.022, 2022.

Reeve, K. A., Boebel, O., Strass, V., Kanzow, T., and Gerdes, R.: Horizontal circulation and volume transports in the Weddell Gyre derived from Argo float data, Progress in Oceanography, 175, 263–283, https://doi.org/10.1016/j.pocean.2019.04.006, 2019.

Ryan, S., Hattermann, T., Darelius, E., and Schröder, M.: Seasonal cycle of hydrography on the eastern shelf of the Filchner Trough, Weddell Sea, Antarctica, Journal of Geophysical Research: Oceans, 122, 6437–6453, https://doi.org/10.1002/2017JC012916, 2017.

Ryan, S., Hellmer, H. H., Janout, M., Darelius, E., Vignes, L., and Schröder, M.: Exceptionally Warm and Prolonged Flow of Warm Deep Water Toward the Filchner-Ronne Ice Shelf in 2017, Geophysical Research Letters, 47, https://doi.org/10.1029/2020GL088119, 2020.

Schaffer, J., Timmermann, R., Arndt, J. E., Kristensen, S. S., Mayer, C., Morlighem, M., and Steinhage, D.: A global, high-resolution data set of ice sheet topography, cavity geometry, and ocean bathymetry, Earth System Science Data, 8, 543–557, https://doi.org/10.5194/essd-8-543-2016, 2016.

Semmler, T., Danilov, S., Gierz, P., Goessling, H. F., Hegewald, J., Hinrichs, C., Koldunov, N., Khosravi, N., Mu, L., Rackow, T., Sein, D. V., Sidorenko, D., Wang, Q., and Jung, T.: Simulations for CMIP6 with the AWI Climate Model AWI-CM-1-1, Journal of Advances in Modeling Earth Systems, 12, 1–34, https://doi.org/10.1029/2019MS002009, 2020.

Talley, L.: Closure of the Global Overturning Circulation Through the Indian, Pacific, and Southern Oceans: Schematics and Transports, Oceanography, 26, 80–97, https://doi.org/10.5670/oceanog.2013.07, 2013.

Tamsitt, V., England, M. H., Rintoul, S. R., and Morrison, A. K.: Residence Time and Transformation of Warm Circumpolar Deep Water on the Antarctic Continental Shelf, Geophysical Research Letters, 48, 1–10, https://doi.org/10.1029/2021GL096092, 2021.

Thompson, A. F., Stewart, A. L., Spence, P., and Heywood, K. J.: The Antarctic Slope Current in a Changing Climate, Reviews of Geophysics, 56, 741–770, https://doi.org/10.1029/2018RG000624, 2018.

Timmermann, R. and Goeller, S.: Response to Filchner–Ronne Ice Shelf cavity warming in a coupled ocean–ice sheet model – Part 1: The ocean perspective, Ocean Science, 13, 765–776, https://doi.org/10.5194/os-13-765-2017, 2017.

Timmermann, R. and Hellmer, H. H.: Southern Ocean warming and increased ice shelf basal melting in the twenty-first and twenty-second centuries based on coupled ice-ocean finite-element modelling, Ocean Dynamics, 63, 1011–1026, https://doi.org/10.1007/s10236-013-0642-0, 2013.

Timmermann, R., Wang, Q., and Hellmer, H.: Ice-shelf basal melting in a global finite-element sea-ice/ice-shelf/ocean model, Annals of Glaciology, 53, 303–314, https://doi.org/10.3189/2012AoG60A156, 2012.

Wang, Q., Danilov, S., Sidorenko, D., Timmermann, R., Wekerle, C., Wang, X., Jung, T., and Schröter, J.: The Finite Element Sea Ice-Ocean Model (FESOM) v.1.4: formulation of an ocean general circulation model, Geoscientific Model Development, 7, 663–693, https://doi.org/10.5194/gmd-7-663-2014, 2014.

Wekerle, C., Krumpen, T., Dinter, T., von Appen, W.-J., Iversen, M. H., and Salter, I.: Properties of Sediment Trap Catchment Areas in Fram Strait: Results From Lagrangian Modeling and Remote Sensing, Frontiers in Marine Science, 5, https://doi.org/10.3389/fmars.2018.00407, 2018.